Integrator-mediated clustering of poised RNA polymerase II synchronizes histone transcription

Feiyue Lu[1], Brandon J. Park[2,†], Rina Fujiwara[3], Jeremy E. Wilusz[3], David S. Gilmour[2], Ruth Lehmann[4,5] and Timothée Lionnet[1,6,7]*

[1]Institute for Systems Genetics, NYU Grossman School of Medicine, New York, NY 10016, USA.
[2]Center for Eukaryotic Gene Regulation, Department of Biochemistry and Molecular Biology, The Pennsylvania State University, University Park, PA 16802, USA.
[3]Verna and Marrs McLean Department of Biochemistry and Molecular Pharmacology, Therapeutic Innovation Center, Baylor College of Medicine, Houston, TX 77030, USA
[4]Whitehead Institute for Biomedical Research, Cambridge, MA 02142, USA.
[5]Department of Biology, Massachusetts Institute of Technology, Cambridge, MA 02139, USA.
[6]Department of Cell Biology, NYU Grossman School of Medicine, New York, NY 10016, USA.
[7]Department of Biomedical Engineering, NYU Tandon School of Engineering, Brooklyn, NY 11201, USA.
[†]Present address: University of Rochester, NY 14642, USA.
*Corresponding author. Email: timothee.lionnet@nyulangone.org

Abstract:
Dynamic clustering of transcription players, including RNA polymerase II (Pol II), is thought to rely on multivalent interactions of their intrinsically disordered regions, thereby enhancing active transcription. Using the histone locus bodies (HLBs) of *Drosophila* nurse cells as a model, we find that Pol II forms long-lived, transcriptionally poised clusters distinct from liquid droplets, which contain unbound and paused Pol II. Depletion of the Integrator complex endonuclease module, but not its phosphatase module or pausing factors disperses these Pol II clusters, leaving HLBs intact. Consequently, histone transcription fails to reach peak levels during S-phase and aberrantly spills over throughout the cell cycle. We propose that clustering sequesters numerous poised Pol II molecules near gene promoters to ensure synchronous and efficient gene activation at desired times.

Introduction:
Numerous regulators of eukaryotic transcription, including the major RNA-synthesizing enzyme, RNA polymerase II (Pol II (*1–9*)), co-activators (*3*, *7*, *10*), as well as general (*7*, *11*, *12*) and sequence-specific transcription factors (*13–15*), can assemble into membrane-less clusters. These clusters are mostly highly dynamic, short-lived, and exhibit liquid-like properties (*16*). Clustering of transcription regulators is dependent on the multivalent interactions of their intrinsically disordered regions (IDRs) and is generally thought to be mediated by liquid-liquid phase separation (LLPS) (*3*, *4*, *10*, *11*, *17*, *18*), although LLPS-independent mechanisms could also be

involved (*19–21*). Since its initial observation, clustering has been thought to facilitate transcription by allowing for the rapid accumulation of high concentrations of regulatory molecules at the target genes (*22*), which is supported by recent observations that artificially induced clustering of transcription factors is sufficient to boost transcription (*23–25*).

Pol II clustering is mediated by the disordered C-terminal domain (CTD) of its largest Rpb1 subunit. Pol II is recruited to transcription sites largely unphosphorylated and is subsequently phosphorylated by CTD kinases at various stages of transcription (*26–29*). *In vitro*, the Pol II CTD alone can partition into hydrogels containing other transcription factor IDRs (*30*), is sufficient to form phase-separated clusters (*31*), and can incorporate into co-activator condensates (*4*), all of which are disrupted upon CTD phosphorylation. *In vivo*, Pol II forms numerous clusters that are liquid-like (*3*), CTD-length dependent (*31*), and correlate with transcription bursts (*2*, *5*). These findings led to the model that Pol II clustering occurs before transcription initiation whereas transcription-coupled phosphorylation of the CTD releases Pol II from clusters and allows for productive elongation (*29–31*). However, whether endogenous Pol II clustering constitutes a regulatory checkpoint in the cellular context remains untested. Here, we leveraged microscopy with genetic perturbations in the *Drosophila* ovarian nurse cells to investigate the dynamics, assembly, and activation of Pol II clustering at the histone locus and its regulatory roles in transcription.

Capturing Pol II clustering at the histone loci of the *Drosophila* nurse cells

Pol II clusters are often short-lived and range in size from diffraction-limited to sub-micron in diameters in most cells (*1–9*), requiring either cutting-edge microscopic technologies for detection at high spatiotemporal resolution or repetitive synthetic gene arrays for signal amplification. The histone loci in the *Drosophila* ovarian nurse cells (NCs) of developing egg chambers provide a unique, natural system for capturing Pol II clustering without the need for either. The NCs are endocycling cells with alternating G and S cycles that can grow to 1,000 n ploidy and reach 50 µm or more in nuclear diameter (*32*) (Fig. 1A). The most prominent Pol II clusters often reside on the replication-dependent histone genes (*6*, *8*, *9*, *33*), which in *Drosophila* are present in ~100 copies at a single locus (*34*). The histone locus self-organizes into membrane-less subnuclear compartments called histone locus bodies (HLBs) (*35*), which form one visible focus per NC in early egg chambers and multiple foci per NC in mid to late-stage egg chambers as DNA copy number increases (*36–38*) (Fig. 1B). The repetitiveness of the *Drosophila* histone loci combined with the polyploidy of NCs thus constitute a naturally occurring signal amplification platform for imaging Pol II clusters.

To image Pol II clustering, we generated a homozygous viable, Halo-tagged Pol II fly line by appending the tag to the C-terminus of the Rpb1 subunit following a previously described

CRISPR/Cas9 editing scheme (*39*). Halo-tagged Rpb1 is expressed at endogenous levels, associates with chromosomes, and responds normally upon heat shock (fig. S1). In NCs from Stage 2 to 9 egg chambers, histone mRNAs are synthesized in S-phase and degrade upon exiting S-phase (*38*). Consistently, micron-sized HLB-bound Pol II clusters (Fig. 1B) are observed in all S-phase NCs (N=109) when histone transcription is active. However, 72% of G-phase NCs (N=150) also contain visible HLB-bound Pol II clusters. Since each endocycle lasts for at least 7 hours in NCs (*32*), Pol II clusters must be present for substantial periods outside the window in which histone transcription takes place. To capture this phenomenon in live egg chambers, we used a fly line that expresses both Halo-Rpb1 and a cell cycle marker GFP-CycE (*32*), which localizes to S-phase HLBs (*35*, *38*) (fig. S2). Indeed, Pol II clusters form before entry into S-phase and persist hours after exiting S-phase (Fig. 1C, movie S1 and S2). The lack of Pol II clusters at the HLBs over a fraction of G-phase is not simply due to dispersion of the HLBs: unlike in tissue-cultured cells or in the early fly embryos where HLBs gradually dissolve during cell division and reform upon mitotic exit (*8*, *35*, *40*), micron-sized HLBs (marked by HLB scaffolding protein Mxc) are present in all NCs regardless of cell cycle stages (*36–38*) (Fig. 1B), presumably due to the lack of cell division. This suggests that there must be separate mechanisms controlling Pol II clustering at HLBs from those regulating HLB assembly. Collectively, the HLBs of NCs provide a highly tractable system that enables the observation of Pol II clustering with high spatiotemporal resolution at a native locus whose transcription activation is tightly coupled to the cell cycle.

The HLB-bound Pol II clusters do not show hallmarks of CTD-driven LLPS

If the formation of HLB-bound Pol II clusters is entirely driven by CTD-dependent LLPS, three predictions should be fulfilled: first, fluorescent Pol II molecules within clusters should exhibit rapid recovery upon bleaching (*3*, *4*, *31*); second, treatment with 1,6-hexanediol (1,6-HD), a chemical sufficient for disrupting weak hydrophobic interactions, should dissolve Pol II clusters (*3*, *4*, *8*, *31*); and third, the propensity of Pol II clustering should increase as the CTD length increases (*31*). Contrary to the first expectation, Pol II exhibited little to no recovery by fluorescence recovery after photobleaching (FRAP) (Fig. 2A). Furthermore, the HLB-bound Pol II clusters survived treatment with 5% 1,6-HD, unlike P-bodies (marked by Me31B-GFP) that were largely dissolved (*41*) (Fig. 2B). Finally, to directly compare the clustering propensity of Pol II molecules containing CTDs varying in length and sequence composition, we mated an endogenously HA-tagged wild-type Rpb1 (HA-Rpb1^{WT}) fly line to various FLAG-tagged Rpb1 CTD variants (*42*) such that the resulting female progenies have a copy of each Pol II form. The stoichiometric ratios of the FLAG variants to HA-Rpb1^{WT} at the HLBs do not increase with increasing CTD length, opposite to the prediction of CTD-dependent LLPS model (Fig. 2C and fig. S3). While we cannot rule out the possibility that LLPS mediates some aspects of Pol II

clustering, these observations argue that additional mechanisms must be involved in the formation of Pol II clusters.

Nearly all the HLB-bound Pol II molecules are transcriptionally inactive

The observation that Pol II clusters are present at the HLBs in the majority of G-phase NCs suggests that a fraction of the Pol II clusters are transcriptionally inactive. To confirm this, we measured Ser2 phosphorylation (Ser2ph) levels at HLBs. Ser2ph marks Pol II molecules that have advanced beyond the promoter-proximal regions of genes (*26*, *28*, *29*). Amongst all NCs analyzed, only 2.9% (N=448) showed visible levels of Ser2ph enrichment over nucleoplasm (Fig. 3A), suggesting that high levels of histone transcription only take place during a tiny fraction of the clustering lifetime. To further validate this, we pulse-labeled egg chambers with 5-ethynyl uridine (EU) to detect nascent transcripts (*43*). Similar to Ser2ph, 3.0% of all NCs (N=311) contained HLB-bound Pol II clusters with detectable levels of EU incorporation (Fig. 3B, lower panels). The low EU enrichment at the HLBs is not due to insufficient sensitivity: besides HLBs, Pol II forms numerous sub-micron clusters in Stage 10 NCs, a fraction of which showed high EU enrichment (Fig. 3B, upper panels, blue arrows). Finally, to investigate whether transcription elongation is required for Pol II clustering at the HLBs, we treated egg chambers with flavopiridol (FP), an inhibitor of the kinase P-TEFb which deposits the Ser2ph mark and releases paused Pol II into productive elongation (*44*). While FP effectively inhibits P-TEFb as indicated by reduced nuclear levels of Ser2ph (fig. S4) (*28*, *45*), Pol II clusters are not dissolved (Fig. 3C, movie S3). Together, these data argue that Pol II clustering occurs before pause release, with most Pol II molecules remaining inactive for a substantial period following recruitment to the HLBs.

The HLB-bound clusters contain both promoter-proximal paused and unbound Pol II molecules

Since the vast majority of HLBs exhibit undetectable levels of productively transcribing Pol II, we next explored the possibility that the Pol II clusters contain promoter-proximal paused Pol II. We reasoned that if we depleted Spt6 or Spt5, two factors that sustain promoter-proximal pausing (*46*, *47*), paused Pol II should be released into the gene body. In consequence, if the HLBs contained paused Pol II, their Ser2ph levels should increase upon Spt6 or Spt5 depletion. Indeed, upon RNAi depletion of Spt6 or Spt5, the levels of Ser2ph drastically increased at the HLBs (Fig. 4A and B, fig. S5 and S6). This suggests that HLB-bound Pol II clusters are at least in part made up of promoter-proximal paused Pol II.

The observation of Pol II clusters highly enriched in Ser2ph upon depletion of pausing factors is seemingly at odds with models suggesting that CTD phosphorylation disrupts Pol II clusters

coincidently with entry into productive elongation (*29–31*). This paradox could be reconciled if upon depletion of pausing factors, Pol II still pauses, but further downstream from the transcription start site. To test this possibility, we pulse-labeled egg chambers with EU and co-stained them for Ser2ph. In control, NCs with detectable levels of both EU uptake and Ser2ph enrichment were rarely observed (2.6%, N=270) and instead almost all nuclei lacked both EU and Ser2ph signals at the HLBs. Upon knockdown of Spt6 or Spt5, we found little EU incorporation at the HLB-bound Pol II clusters despite significant increases in the levels of Ser2ph (fig. S7). This suggests that the promoter-proximal escaped Pol II molecules are stalled further downstream on the template, consistent with recent observations in the case of Spt5 (*47*).

Because Pol II levels at the HLBs do not substantially decrease upon disruption of pausing by Spt6 or Spt5 RNAi, we wondered whether other forms of Pol II besides paused Pol II might be present at the HLBs – for instance unbound Pol II, defined here as Pol II molecules recruited to the vicinity of the promoter but not engaged in the pre-initiation complex or subsequent steps. As Pol II molecules transit from the unbound state to early initiation, their levels of Ser5 phosphorylation (Ser5ph) rapidly increase (*26*, *28*, *29*). We reasoned that treating egg chambers with the initiation inhibitor Triptolide (TRI) should only leave at the HLB stably paused Pol II (*48*), which has higher Ser5ph levels than unbound Pol II. If HLBs are solely constituted of Pol II molecules engaged at 5'-end of genes in unperturbed conditions, we should therefore observe little change in the Ser5ph:Pol II ratio at the HLB upon TRI treatment. Previous studies on Pol II dynamics showed that TRI treatment either completely abolished Pol II clusters (*49*) or led to reduced Pol II intensity at a locus (*5*). Consistent with these observations, the intensity of Pol II clusters at the HLBs drastically decreased irrespective of the cell cycle stages within 35 min of TRI treatment (Fig. 4C, movie S4 and fig. S8), and this decrease was not due to Pol II degradation (fig. S9). Despite a decrease in absolute Ser5ph intensity following TRI treatment (fig. S8), the ratios of Ser5ph:Pol II increased by nearly two-fold after normalizing by nuclear levels (Fig. 4D), suggesting that unbound Pol II molecules are also present at the HLBs in unperturbed conditions.

The Integrator endonuclease module is required for Pol II clustering at the HLBs

In addition to Spt6 and Spt5, we also examined if Integrator, a multi-subunit complex involved in promoter-proximal regulation of transcription, mediates Pol II clustering at the HLBs. The Integrator complex consists of a phosphatase module and an endonuclease module and has been shown to have both activating and repressive roles in the transcription of protein-coding genes (*50–53*). RNAi depletion of IntS8, a key bridging subunit connecting the phosphatase module to the rest of the Integrator, (*54*, *55*) led to increased levels of nuclear Ser5ph including at HLBs (fig. S10), consistent with previous studies (*53*, *55*, *56*). However, the intensity of Pol II at the HLBs did not decrease upon IntS8 RNAi (fig. S10) despite increased Ser5ph, suggesting

hyper-phosphorylation at the Ser5 residues of the Pol II is insufficient to dissolve Pol II clusters. In contrast to IntS8, RNAi depletion of the Integrator endonuclease subunits IntS11 or IntS9 resulted in a complete loss of visible HLB-bound Pol II clusters in all NCs starting from Stage 6 (Fig. 5A and B, and fig. S11). Importantly, the loss of Pol II clusters upon IntS11 or IntS9 RNAi is not simply due to a global loss of HLB structure, as the scaffolding protein Mxc and P-TEFb remained present at the HLBs (fig. S12). Nor is it due to RNAi-induced cell death, as IntS11 RNAi and IntS9 RNAi egg chambers did not show arrested development until Stages 10 and 9, respectively (fig. S13). Collectively, these results establish the Integrator endonuclease module, but not its phosphatase module, as an essential regulator for Pol II clustering at the HLBs.

Inhibition of P-TEFb stimulates clustering of Pol II in the absence of IntS11

Across the literature, P-TEFb has been proposed to play different roles in Pol II clustering. P-TEFb inhibition can lead to the loss of Pol II clusters (*3*, *5*, *57*), which is likely attributed to the blockage in pause release (*45*) if a cluster is mainly made up of high levels of elongating Pol II (*57*). In other contexts, P-TEFb inhibition displays neutral (*4*) to positive effects (*2*, *58*) on Pol II clustering, the latter of which is consistent with the idea that phosphorylation releases Pol II molecules from clusters for productive elongation (*29–31*).

To explore whether P-TEFb inhibition is sufficient to promote Pol II clustering in the absence of the Integrator endonuclease, we treated IntS11-depleted egg chambers with FP. Treatment with FP stimulated the formation of Pol II clusters, despite displaying lower Pol II intensity compared to the control genotype (Fig. 5A and B). To determine the state of "reclustered" Pol II induced by FP, we compared the Ser5ph:Pol II ratios at the HLBs in control versus IntS11 RNAi NCs for both mock-treated and FP-treated conditions. While treatment with FP increased Pol II enrichment at the HLBs, the Ser5ph enrichment was even greater, resulting in a higher Ser5ph:Pol II ratio indicative of a disproportionate increase in 5'-engaged Pol II molecules over unbound ones. In contrast, the Ser5ph:Pol II ratio in the "reclustered" Pol II was comparable to that in the mock-treated IntS11-depleted NCs and lower compared to that in the FP-treated NCs of the control genotype (Fig. 5A and C), suggesting that the "reclustered" Pol II is not simply an accumulation of paused Pol II molecules and consists at least in part of unbound ones. This argues that P-TEFb negatively modulates Pol II clustering separately from its roles in pause release (*45*).

Out-of-phase and reduced hyper-induction of histone transcription upon loss of the Integrator endonuclease

We next sought to investigate how the loss of Pol II clusters impacts the level and timing of histone transcription. Since Integrator depletion leaves the HLB scaffold intact (Fig. 5 and fig.

S12), any subsequent transcription changes should stem directly from the loss of Pol II clustering rather than changes in the underlying HLB structure. To visualize histone expression, we performed RNA fluorescence in situ hybridization (FISH) against H3 transcripts using highly sensitive hybridization chain reaction (HCR) based methods (*59*). Distinct H3 FISH spots can be seen both at the HLBs and in the cytoplasm nearly exclusively in S-phase NCs (Fig. 6A). To determine whether the HLB-bound H3 FISH spots correspond to nascent transcripts, we combined a single probe against the 5'-end of H3 (*6*) in a first color with a set of probes against the 3'-end of H3 in another color, reasoning that nascent transcripts would only be labeled by the first probe, while full-length counterparts would be labeled in both colors (fig. S14A). We validated this approach in primordial germ cells (PGCs), in which Pol II is initially paused, and then released at later embryonic stages. As expected, the 5'-H3 probe labels all PGCs regardless of embryonic stages whereas the 3'-H3 probe set only labels PGCs at later stages (fig. S14B and C). In NCs, the ratios of the 5'- to 3'-H3 probes are comparable at the HLBs and at cytoplasmic foci (fig. S14D), indicating that most H3 transcripts detected at the HLBs are full-length transcripts. Additionally, treatment with FP for 60 min does not eliminate 3'-H3 signal at the HLBs (fig. S14E), suggesting that full-length histone transcripts likely linger at the HLBs long after transcription terminates.

In agreement with a previous study in *Drosophila* NCs (*38*), H3 transcripts can normally be detected with 3'-H3 probes in all the S-phase NCs but rarely in the G-phase NCs up to Stage 9 (Fig. 6A). Consistent with a low percentage of NCs showing Ser2ph staining at the HLBs or EU uptake (Fig. 3A and B), S-phase NCs with extremely high 3'-H3 signal (z-score>2) were observed in 4.5% (9 out of 201) of all NCs (Fig. 6B). RNAi depletion of IntS11 or IntS9 resulted in a narrower range of H3 expression, with a reduced higher quantile indicative of decreased levels of hyper-induction and an increased lower quantile compared to control (Fig. 6B and fig. S16B). The latter could be attributed to either increased levels of H3 expression in G-phase NCs, increased percentages of S-phase NCs, or both. To eliminate any potential effects of cell cycle disruption, we focused on G-phase NCs and found that the majority showed aberrant H3 expression upon IntS11 and IntS9 RNAi (Fig. 6C, fig. S15 and fig. S16C). In contrast, RNAi depletion of Spt6 or Spt5 resulted in overall reduced expression but not aberrant expression in G-phase (fig. S17), suggesting that the leaky expression cannot be explained by the loss of promoter-proximal Pol II molecules.

The increased level of H3 mRNA in G-phase upon IntS11 and IntS9 RNAi can be triggered by either aberrant activation of histone transcription or disruption of histone mRNA degradation. We first examined the cytoplasmic mRNA levels of the ribosomal protein gene RpL30 and found that it does not display similar levels of increase upon either IntS11 or IntS9 RNAi (Fig. 6A and D and fig. S16A and D), arguing that IntS11 and IntS9 RNAi did not disrupt general mRNA degradation pathways. Since histone transcripts are normally rapidly degraded upon exiting

S-phase, and misprocessing of histone transcripts can lead to downstream degradation defects (*60*), we next investigated whether H3 mRNA is misprocessed upon IntS11 and IntS9 RNAi. In *Drosophila*, histone mRNA 3'-end processing consists of a cleavage step tightly coupled to transcription termination. Unprocessed histone transcripts can therefore be detected using mRNA FISH probes targeting regions downstream of the H3 pre-mRNA cleavage site (*35*, *38*) (Fig. 6E). In control NCs, the downstream H3 probe (DS-H3) detects unprocessed H3 transcripts at the HLBs, consistent with observations in early embryos (*35*). H3 mRNA forms foci in the cytoplasm, which are marked by a probe against the H3 gene body (3'-H3), but not by the DS-H3 probe. The ratios of DS-H3 to 3'-H3 signals did not increase at the HLBs nor in the cytoplasm upon IntS11 or IntS9 RNAi (Fig. 6F and G, fig. S16E and F), thus ruling out the effects of misprocessing on misexpression. Together, these results argue that the misexpression of H3 in G-phase upon depletion of the Integrator endonuclease is due to aberrant transcription activation.

Discussion

Transcription activators including Pol II are thought to cluster via multivalent interactions of their IDRs, which in turn might facilitate transcription through mass action (*22–25*, *61*). While several recent studies have demonstrated that artificially induced clustering of transcription activators at some loci is indeed sufficient to drive transcription (*23–25*), others have also shown that artificially induced clustering does not activate (*20*) or can even repress transcription (*21*). Yet it remains unclear whether artificial clusters recapitulate the size or organization of physiological clusters, leaving unanswered the question of the function of clustering in the endogenous context. Our observation that endogenous clustering of Pol II at the HLBs can occur without histone transcription argues against the simple model of clustering-facilitated transcription. Furthermore, HLB-bound Pol II clusters do not show hallmarks of CTD-driven LLPS and persist in the presence of hyper-phosphorylation at either Ser2 or Ser5 residues of the CTD. This suggests that clustering must be subjected to additional layers of regulation beyond CTD-phosphorylation-gated phase separation.

The identification of the Integrator endonuclease module as a regulator of Pol II clustering allows us to test the essentiality of Pol II clustering in normal physiology and reveals opposing functions at the histone locus across different cell cycle stages: In S-phase, loss of clustering reduces the level of transcription induction, consistent with models proposing activating functions by increasing local concentrations (*22–25*). In G-phase, however, loss of clustering leads to aberrant histone transcription, suggestive of its repressive role in transcription. Hence, we propose that clustering ensures synchronous and robust transcription by enabling the accumulation of large quantities of poised Pol II molecules that can be activated at designated times (Fig. 7). While we do not know what switches Pol II clusters from the poised to active states, the observation that

Pol II clusters are present without active histone transcription argues that the maintenance of Pol II clustering and transcription activation must be regulated separately. Coincidentally, a recent study shows that only a fraction of the Notch transcription hubs can progress to a state of transcription activation upon signaling induction (*62*), suggesting the stepwise control mechanism we observed constitutes a general regulatory architecture.

The Integrator endonuclease is required for the promoter-proximal termination of many genes (*50–53*) but whether it ultimately activates or represses transcription has been a subject of debate. IntS11 can facilitate pause release (*52*, *63–65*), presumably by evicting stalled Pol II on genes; alternatively, it can attenuate transcription by terminating elongation-competent Pol II (*66*, *67*). Recent genome-wide analyses (*53*, *68*) revealed differential effects across various protein-coding genes upon depleting IntS11, with highly expressed genes showing downregulation and lowly expressed genes showing upregulation (*53*). Mechanisms underlying the differential regulation remain largely elusive, although it was speculated that IntS11 might preferentially target stalled Pol II at highly expressed promoters where endonuclease activity is more limiting (*53*). Our finding that the Integrator endonuclease module is an essential clustering regulator offers a possible resolution to this conundrum: depletion of the Integrator endonuclease results in the loss of Pol II clusters but its downstream transcriptional effects may depend on whether the Pol II clusters are activated or poised at the time of depletion: for the highly expressed promoters (as was the case with the highly activated S-phase histone loci) where the Pol II clusters are more likely to be active, loss of Pol II clustering would lead to transcriptional downregulation; for the lowly expressed promoters (as was the case with all the G-phase histone loci), loss of clustering would bypass the regulatory transition from poised to activation, causing aberrant transcriptional activation.

Finally, “poised for activation” has long been proposed to be a function of promoter-proximal pausing of Pol II (*69–75*). While the Pol II clusters at the HLBs consist of both unbound and paused Pol II molecules, depletion of pausing factors Spt6 and Spt5 did not result in leaky histone expression, suggesting that promoter-proximal pausing alone is insufficient to explain the effects of clustering regulation. In summary, our study presents direct evidence that Pol II clustering is a rate-limiting step in transcription and sheds light on Integrator functions as well as promoter-proximal regulation.

Acknowledgments: We thank Robert Duronio (UNC-Chapel Hill) for the GFP-mxc fly line and anti-Mxc antibody, Elizabeth Gavis (Princeton) for the GFP-CycE fly line, Akira Nakamura (RIKEN) for anti-CycT antibody, John Lis (Cornell) for anti-Spt6 antibody, Stefano Di Talia (Duke) for discussion on the DS-H3 HCR FISH probe design, Luke Lavis (Janelia) for the JF dyes. Eric Wagner (URMC), Yu Cai (NUS), and Patrick O’Farrell (UCSF) for critical reagents,

Yujun Chen (K-State) for *ex-vivo* ovary culture advice, Nicholas Mamrak for designing the 5'- and 3'-H3 HCR FISH probes, Eli Rothenberg's lab (NYU Langone) for assistance with EU labeling, NYU Langone Health Microscopy Laboratory (RRID: SCR_017934) Michael Cammer and Yan Deng for consultation and assistance with optical microscopy services, the TRiP at Harvard Medical School for providing various RNAi fly stocks used in this study, the Lionnet and Lehmann lab members for comments.

Funding:

National Institutes of Health grant R01 AG075272 to T.L.

National Institutes of Health grant R01 HD110546-01 to R.L.

National Institutes of Health grant R01 GM047477 to D.S.G.

National Institutes of Health grant R35 GM119735 to J.E.W.

Cancer Prevention & Research Institute of Texas grant RR210031 to J.E.W. J.E.W. is a CPRIT Scholar Cancer Research.

Microscopy shared resource is partially supported by the Cancer Center Support Grant, P30CA016087.

NYSTEM Institutional Training Grant #C032560GG to F.L.

Author contributions: F.L. conceived the project. T.L. and R.L. co-supervised the project. F.L., R.L., and T.L. designed experiments. B.J.P. performed Pol II CTD mutational analyses and contributed to crucial preliminary data. R.F. and J.E.W. designed and generated the *Drosophila* IntS8 antibody. D.S.G. generated the Halo-Rpb1 fly line and supported the initial phase of the project. F.L. performed all other experiments. F.L. and T.L. analyzed the data. F.L., R.L., and T.L. interpreted the data. F.L. drafted the manuscript. F.L. T.L., R.L., D.S.G., J.E.W., and B.J.P. revised the manuscript.

Fig. 1. Micron-sized Pol II clusters are present at the HLBs of the *Drosophila* NCs both during and outside of the S-phase. (**A**) A schematic of a developing ovariole, which contains egg chambers of increasing maturity from anterior to posterior. Each egg chamber consists of 15 NCs and an oocyte (dark gray). All experiments in this study are performed in NCs between Stages 5 and 10 (boxed region) when the nuclei grow from 10 µm to above 50 µm in diameter. (**B**) Upper: 3D rendering of a Stage 6 egg chamber expressing the HLB marker GFP-mxc and Halo-tagged Rpb1. Lower: Z projection of the boxed region in the upper panel showing two nuclei, one of which has distinct Pol II clusters present at the HLBs. The scale bar represents 5 µm. (**C**) Time-lapse movies of two nuclei that are entering (upper) and exiting (lower) the S-phase respectively. CycE-GFP is a cell-cycle marker (*32*). See also fig. S2. Time 0 represents the start of the S-phase (upper) and the G-phase (lower) respectively. Halo-Rpb1 was labeled by Janelia Fluor 549 (JF549) (*76*). The scale bar represents 10 µm.

Fig. 2. The HLB-bound Pol II clusters show slow recovery in FRAP, are insensitive to hexanediol, and do not show more clustering at increased CTD lengths. (**A**) Two examples from FRAP experiments targeting HLB-bound Pol II clusters. The yellow arrows indicate bleached clusters. The upper cluster showed partial recovery after 60 minutes whereas the lower cluster did not show any detectable level of recovery after 120 minutes. The scale bar represents 5 µm. (**B**) Treatment with 5% 1,6-hexanediol for 20 min dissolves P-bodies (marked by me31-GFP) but not Pol II clusters. The scale bar represents 10 µm. (**C**) Normalized intensity of Pol II CTD variants at the HLBs. Each dot represents the ratio of FLAG-tagged Pol II CTD variants to HA-tagged wild-type (WT) Pol II at HLBs, averaged across one nucleus (normalized by expression). The WT *Drosophila* Pol II CTD contains 42 repeats, most of which are variants of the consensus YSPTSPS motif. Pol II CTD variants contain 20, 29, 42, and 52 precise copies of YSPTSPS (*42*). Error bars represent mean ± SEM. Data was acquired from at least 4 female flies per genotype. P-values (compared to WT): P<0.0001 (20X), P=0.2673 (29X), P=0.1157 (42X), P=0.5792 (52X). See also Materials and Methods and fig. S3.

Fig. 3. Most HLB-bound Pol II clusters lack detectable levels of Ser2ph and EU and are not dispersed when elongation is inhibited. (**A**) Representative images of HLB-bound Pol II clusters scored negative (Example 1) or positive (Example 2) for Ser2ph staining. (**B**) Representative images of HLB-bound Pol II clusters scored negative (Example 1) or positive (Example 2) for EU incorporation. HLBs are marked by yellow arrows; blue arrows mark small EU-rich foci. Nucleoli also showed strong EU enrichment consistent with their role in rRNA synthesis. (**C**) The HLB-bound Pol II clusters survived a 1-hour treatment with 500 nM FP. Halo-Rpb1 was labeled by Janelia Fluor 646 (JF646) (*76*). Scale bars represent 10 µm.

Fig. 4. Both promoter-proximal paused and unbound Pol II molecules are present at the HLB-bound clusters. (**A**) RNAi depletion of Spt6 and Spt5 results in increased levels of Ser2ph at the HLBs. mCherry-RNAi serves as a negative control. The scale bar represents 5 µm. (**B**) Quantification of Ser2ph levels at HLBs. Each dot represents one NC. Error bars represent mean ± SEM. Data was collected from 11, 5, and 6 egg chambers (from at least 3 females per genotype) for mCherry RNAi, Spt6 RNAi, and Spt5 RNAi respectively. P-values (compared to *mCherry-RNAi*): P<0.0001 (*Spt6-RNAi*), P=0.0158 (*Spt5-RNAi*). See also fig. S6. (**C**) 35 min of 500 µM TRI treatment results in decreased levels of Pol II and Ser5ph at the HLBs. Halo-Rpb1 was labeled by JF646. The scale bar represents 10 µm. (**D**) Quantification of the Ser5ph:Pol II ratios at the HLBs in DMSO-treated versus TRI-treated NCs, grouped by cell cycle stages. Each dot represents the average Ser5ph:Pol II ratio in one egg chamber. Error bars represent mean ± SEM. Data was stage-matched and acquired from at least 6 female flies per condition. The levels of Ser5ph and Pol II were normalized by their nuclear levels. P-values (DMSO-treated versus TRI-treated): P<0.0001 (G-phase), P<0.0001 (S-phase). See also Materials and Methods and fig. S8.

Fig. 5. Depletion of IntS11 eliminates all HLB-bound Pol II clusters, which can be partially restored by inhibiting P-TEFb. (**A**) RNAi depletion of IntS11 results in complete loss of Pol II clusters at the HLBs, which is partially restored by 1-hour treatment of 500 nM FP. P-TEFb is enriched at the HLBs during the S-phase (see also fig. S12), which serves as a cell cycle marker. mCherry-RNAi serves as a negative control. The scale bar represents 5 μm. (**B** and **C**) Quantification of the levels of Pol II (B) and Ser5ph:Pol II ratios (C) at the S-phase HLBs (demarcated by MPM-2). Each dot represents the measurement in one egg chamber. The Ser5ph:Pol II ratio increased 92.46% in FP-treated versus DMSO-treated condition in the mCherry RNAi control but only increased 6.55% upon IntS11 RNAi (C). Error bars represent mean ± SEM. All data was stage-matched and acquired from at least 6 female flies per condition. The levels of Ser5ph and Pol II were normalized by their nuclear levels. P-values: For (B), P=0.0069 (*mCherry-RNAi*, DMSO vs FP), P<0.0001 (*IntS11-RNAi*, DMSO vs FP). P<0.0001 (FP, *mCherry-RNAi* vs *IntS11-RNAi*). For (C), P<0.0001 (*mCherry-RNAi*, DMSO vs FP), P=0.0342 (*IntS11-RNAi*, DMSO vs FP). See also Materials and Methods.

Fig. 6. Depletion of IntS11 results in reduced hyper-induction and out-of-phase histone transcription. (**A**) Representative images showing egg chambers probed with MPM-2 (S-phase marker), H3 mRNA, and RpL30 mRNA (control). mCherry-RNAi serves as a negative control. Green arrows point at the S-phase NCs whereas magenta and yellow arrows point at the G-phase NCs without and with H3 mRNA respectively. (**B**) Quantification of the cytoplasmic H3 mRNA intensity. Each dot represents one NC. Bars represent quantiles. (**C**) Quantification of % of MPM-2 negative NCs with cytoplasmic H3 mRNA signals. n=75 (*mCherry-RNAi*), n=94 (*IntS11-RNAi*). P<0.0001 (two-sided chi-square test). See also fig. S15. (**D**) Quantification of cytoplasmic RpL30 mRNA. Each dot represents the average mRNA level in one egg chamber. Error bars represent mean ± SEM. P=0.6671. (**E**) A schematic showing the design of downstream H3 (DS-H3) probe for detection of unprocessed H3 mRNA, adapted from (*35*). (**F**) Representative images showing NCs probed with both the 3'-H3 and DS-H3 FISH probes. DNA was detected by Hoechst as a reference for the nuclei. (**G**) Quantification of DS-H3 to 3'-H3 mRNA ratios at the HLBs and the mRNA clusters in the cytoplasm. Each dot represents one NC. Error bars represent mean ± SEM. P-values (*mCherry-RNAi* vs *IntS11-RNAi*): P=0.2485 (HLB particles), P=0.5439 (cytoplasmic particles). All data was stage-matched and acquired from at least 6 female flies per genotype. Scale bars represent 10 μm.

Fig. 7. Model for clustering-regulated transcription at the replication-dependent histone loci. Poised and elongating Pol II molecules are marked in blue and orange respectively. Normally, Pol II molecules start to form clusters during the G-phase and remain inactive near promoters until they are licensed for transcription during the S-phase. In the absence of the Integrator endonuclease, clustering-regulated transcription is lost. As a result, Pol II becomes elongation-competent once recruited to the promoters, leading to "leaky" histone transcription in G-phase as well as reduced histone transcription induction in S-phase.

References:

1. I. I. Cisse, I. Izeddin, S. Z. Causse, L. Boudarene, A. Senecal, L. Muresan, C. Dugast-Darzacq, B. Hajj, M. Dahan, X. Darzacq, Real-Time Dynamics of RNA Polymerase II Clustering in Live Human Cells. *Science*. **341** (2013), pp. 664–667.

2. W.-K. Cho, N. Jayanth, B. P. English, T. Inoue, J. O. Andrews, W. Conway, J. B. Grimm, J.-H. Spille, L. D. Lavis, T. Lionnet, I. I. Cisse, RNA Polymerase II cluster dynamics predict mRNA output in living cells. *Elife*. **5** (2016), doi:10.7554/eLife.13617.

3. W.-K. Cho, J.-H. Spille, M. Hecht, C. Lee, C. Li, V. Grube, I. I. Cisse, Mediator and RNA polymerase II clusters associate in transcription-dependent condensates. *Science*. **361**, 412–415 (2018).

4. Y. E. Guo, J. C. Manteiga, J. E. Henninger, B. R. Sabari, A. Dall'Agnese, N. M. Hannett, J.-H. Spille, L. K. Afeyan, A. V. Zamudio, K. Shrinivas, B. J. Abraham, A. Boija, T.-M. Decker, J. K. Rimel, C. B. Fant, T. I. Lee, I. I. Cisse, P. A. Sharp, D. J. Taatjes, R. A. Young, Pol II phosphorylation regulates a switch between transcriptional and splicing condensates. *Nature*. **572**, 543–548 (2019).

5. J. Li, A. Dong, K. Saydaminova, H. Chang, G. Wang, H. Ochiai, T. Yamamoto, A. Pertsinidis, Single-Molecule Nanoscopy Elucidates RNA Polymerase II Transcription at Single Genes in Live Cells. *Cell*. **178**, 491–506.e28 (2019).

6. S.-K. Huang, P. H. Whitney, S. Dutta, S. Y. Shvartsman, C. A. Rushlow, Spatial organization of transcribing loci during early genome activation in Drosophila. *Curr. Biol.* **31**, 5102–5110.e5 (2021).

7. V. Q. Nguyen, A. Ranjan, S. Liu, X. Tang, Y. H. Ling, J. Wisniewski, G. Mizuguchi, K. Y. Li, V. Jou, Q. Zheng, L. D. Lavis, T. Lionnet, C. Wu, Spatiotemporal coordination of transcription preinitiation complex assembly in live cells. *Mol. Cell*. **81**, 3560–3575.e6 (2021).

8. T. Imada, T. Shimi, A. Kaiho, Y. Saeki, H. Kimura, RNA polymerase II condensate formation and association with Cajal and histone locus bodies in living human cells. *Genes Cells*. **26**, 298–312 (2021).

9. C.-Y. Cho, J. P. Kemp Jr, R. J. Duronio, P. H. O'Farrell, Coordinating transcription and replication to mitigate their conflicts in early Drosophila embryos. *Cell Rep.* **41**, 111507 (2022).

10. B. R. Sabari, A. Dall'Agnese, A. Boija, I. A. Klein, E. L. Coffey, K. Shrinivas, B. J. Abraham, N. M. Hannett, A. V. Zamudio, J. C. Manteiga, C. H. Li, Y. E. Guo, D. S. Day, J. Schuijers, E. Vasile, S. Malik, D. Hnisz, T. I. Lee, I. I. Cisse, R. G. Roeder, P. A. Sharp, A. K. Chakraborty, R. A. Young, Coactivator condensation at super-enhancers links phase separation and gene control. *Science*. **361** (2018), doi:10.1126/science.aar3958.

11. H. Lu, D. Yu, A. S. Hansen, S. Ganguly, R. Liu, A. Heckert, X. Darzacq, Q. Zhou,

Phase-separation mechanism for C-terminal hyperphosphorylation of RNA polymerase II. *Nature*. **558**, 318–323 (2018).

12. P. Rawat, M. Boehning, B. Hummel, F. Aprile-Garcia, A. S. Pandit, N. Eisenhardt, A. Khavaran, E. Niskanen, S. M. Vos, J. J. Palvimo, A. Pichler, P. Cramer, R. Sawarkar, Stress-induced nuclear condensation of NELF drives transcriptional downregulation. *Mol. Cell*. **81**, 1013–1026.e11 (2021).

13. M. Mir, A. Reimer, J. E. Haines, X.-Y. Li, M. Stadler, H. Garcia, M. B. Eisen, X. Darzacq, Dense Bicoid hubs accentuate binding along the morphogen gradient. *Genes Dev.* **31**, 1784–1794 (2017).

14. S. Chong, C. Dugast-Darzacq, Z. Liu, P. Dong, G. M. Dailey, C. Cattoglio, A. Heckert, S. Banala, L. Lavis, X. Darzacq, R. Tjian, Imaging dynamic and selective low-complexity domain interactions that control gene transcription. *Science*. **361** (2018), doi:10.1126/science.aar2555.

15. M. Mir, M. R. Stadler, S. A. Ortiz, C. E. Hannon, M. M. Harrison, X. Darzacq, M. B. Eisen, Dynamic multifactor hubs interact transiently with sites of active transcription in Drosophila embryos. *Elife*. **7** (2018), doi:10.7554/eLife.40497.

16. F. Lu, T. Lionnet, Transcription Factor Dynamics. *Cold Spring Harb. Perspect. Biol.* **13** (2021), doi:10.1101/cshperspect.a040949.

17. A. Boija, I. A. Klein, B. R. Sabari, A. Dall'Agnese, E. L. Coffey, A. V. Zamudio, C. H. Li, K. Shrinivas, J. C. Manteiga, N. M. Hannett, B. J. Abraham, L. K. Afeyan, Y. E. Guo, J. K. Rimel, C. B. Fant, J. Schuijers, T. I. Lee, D. J. Taatjes, R. A. Young, Transcription Factors Activate Genes through the Phase-Separation Capacity of Their Activation Domains. *Cell*. **175**, 1842–1855.e16 (2018).

18. H. Lyons, R. T. Veettil, P. Pradhan, C. Fornero, N. De La Cruz, K. Ito, M. Eppert, R. G. Roeder, B. R. Sabari, Functional partitioning of transcriptional regulators by patterned charge blocks. *Cell*. **186**, 327–345.e28 (2023).

19. D. T. McSwiggen, A. S. Hansen, S. S. Teves, H. Marie-Nelly, Y. Hao, A. B. Heckert, K. K. Umemoto, C. Dugast-Darzacq, R. Tjian, X. Darzacq, Evidence for DNA-mediated nuclear compartmentalization distinct from phase separation. *Elife*. **8** (2019), doi:10.7554/eLife.47098.

20. J. Trojanowski, L. Frank, A. Rademacher, N. Mücke, P. Grigaitis, K. Rippe, Transcription activation is enhanced by multivalent interactions independent of phase separation. *Mol. Cell*. **82**, 1878–1893.e10 (2022).

21. S. Chong, T. G. W. Graham, C. Dugast-Darzacq, G. M. Dailey, X. Darzacq, R. Tjian, Tuning levels of low-complexity domain interactions to modulate endogenous oncogenic transcription. *Mol. Cell*. **82**, 2084–2097.e5 (2022).

22. A. J. Plys, R. E. Kingston, Dynamic condensates activate transcription. *Science*. **361** (2018),

pp. 329–330.

23. M.-T. Wei, Y.-C. Chang, S. F. Shimobayashi, Y. Shin, A. R. Strom, C. P. Brangwynne, Nucleated transcriptional condensates amplify gene expression. *Nat. Cell Biol.* **22**, 1187–1196 (2020).

24. N. Schneider, F.-G. Wieland, D. Kong, A. A. M. Fischer, M. Hörner, J. Timmer, H. Ye, W. Weber, Liquid-liquid phase separation of light-inducible transcription factors increases transcription activation in mammalian cells and mice. *Sci Adv*. **7** (2021), doi:10.1126/sciadv.abd3568.

25. Y. J. Kim, M. Lee Jr, Y.-T. Lee, J. Jing, J. T. Sanders, G. A. Botten, L. He, J. Lyu, Y. Zhang, M. Mettlen, P. Ly, Y. Zhou, J. Xu, Light-activated macromolecular phase separation modulates transcription by reconfiguring chromatin interactions. *Sci Adv*. **9**, eadg1123 (2023).

26. D. Eick, M. Geyer, The RNA polymerase II carboxy-terminal domain (CTD) code. *Chem. Rev.* **113**, 8456–8490 (2013).

27. J. L. Corden, RNA polymerase II C-terminal domain: Tethering transcription to transcript and template. *Chem. Rev.* **113**, 8423–8455 (2013).

28. J. Zaborowska, S. Egloff, S. Murphy, The pol II CTD: new twists in the tail. *Nat. Struct. Mol. Biol.* **23**, 771–777 (2016).

29. K. M. Harlen, L. S. Churchman, The code and beyond: transcription regulation by the RNA polymerase II carboxy-terminal domain. *Nat. Rev. Mol. Cell Biol.* **18**, 263–273 (2017).

30. I. Kwon, M. Kato, S. Xiang, L. Wu, P. Theodoropoulos, H. Mirzaei, T. Han, S. Xie, J. L. Corden, S. L. McKnight, Phosphorylation-regulated binding of RNA polymerase II to fibrous polymers of low-complexity domains. *Cell*. **155**, 1049–1060 (2013).

31. M. Boehning, C. Dugast-Darzacq, M. Rankovic, A. S. Hansen, T. Yu, H. Marie-Nelly, D. T. McSwiggen, G. Kokic, G. M. Dailey, P. Cramer, X. Darzacq, M. Zweckstetter, RNA polymerase II clustering through carboxy-terminal domain phase separation. *Nat. Struct. Mol. Biol.* (2018), doi:10.1038/s41594-018-0112-y.

32. C. A. Doherty, R. Diegmiller, M. Kapasiawala, E. R. Gavis, S. Y. Shvartsman, Coupled oscillators coordinate collective germline growth. *Dev. Cell*. **56**, 860–870.e8 (2021).

33. B. Guglielmi, N. La Rochelle, R. Tjian, Gene-specific transcriptional mechanisms at the histone gene cluster revealed by single-cell imaging. *Mol. Cell*. **51**, 480–492 (2013).

34. D. J. McKay, S. Klusza, T. J. R. Penke, M. P. Meers, K. P. Curry, S. L. McDaniel, P. Y. Malek, S. W. Cooper, D. C. Tatomer, J. D. Lieb, B. D. Strahl, R. J. Duronio, A. G. Matera, Interrogating the function of metazoan histones using engineered gene clusters. *Dev. Cell*. **32**, 373–386 (2015).

35. W. Hur, J. P. Kemp Jr, M. Tarzia, V. E. Deneke, W. F. Marzluff, R. J. Duronio, S. Di Talia, CDK-Regulated Phase Separation Seeded by Histone Genes Ensures Precise Growth and Function of Histone Locus Bodies. *Dev. Cell*. **54**, 379–394.e6 (2020).

36. Z. F. Nizami, S. Deryusheva, J. G. Gall, Cajal bodies and histone locus bodies in Drosophila and Xenopus. *Cold Spring Harb. Symp. Quant. Biol.* **75**, 313–320 (2010).

37. J.-L. Liu, C. Murphy, M. Buszczak, S. Clatterbuck, R. Goodman, J. G. Gall, The Drosophila melanogaster Cajal body. *J. Cell Biol.* **172**, 875–884 (2006).

38. J. M. Potter-Birriel, G. B. Gonsalvez, W. F. Marzluff, A region of SLBP outside the mRNA-processing domain is essential for deposition of histone mRNA into the Drosophila egg. *J. Cell Sci.* **134** (2021), doi:10.1242/jcs.251728.

39. F. Lu, D. S. Gilmour, Genetic analysis of the RNA polymerase II CTD in Drosophila. *Methods*. **159-160**, 129–137 (2019).

40. C. Armstrong, V. J. Passanisi, H. M. Ashraf, S. L. Spencer, Cyclin E/CDK2 and feedback from soluble histone protein regulate the S phase burst of histone biosynthesis. *Cell Rep.* **42**, 112768 (2023).

41. M. Sankaranarayanan, R. J. Emenecker, E. L. Wilby, M. Jahnel, I. R. E. A. Trussina, M. Wayland, S. Alberti, A. S. Holehouse, T. T. Weil, Adaptable P body physical states differentially regulate bicoid mRNA storage during early Drosophila development. *Dev. Cell*. **56**, 2886–2901.e6 (2021).

42. F. Lu, B. Portz, D. S. Gilmour, The C-Terminal Domain of RNA Polymerase II Is a Multivalent Targeting Sequence that Supports Drosophila Development with Only Consensus Heptads. *Mol. Cell*. **73**, 1232–1242.e4 (2019).

43. C. Y. Jao, A. Salic, Exploring RNA transcription and turnover in vivo by using click chemistry. *Proc. Natl. Acad. Sci. U. S. A.* **105**, 15779–15784 (2008).

44. S. H. Chao, D. H. Price, Flavopiridol inactivates P-TEFb and blocks most RNA polymerase II transcription in vivo. *J. Biol. Chem.* **276**, 31793–31799 (2001).

45. K. Fujinaga, F. Huang, B. M. Peterlin, P-TEFb: The master regulator of transcription elongation. *Mol. Cell*. **83**, 393–403 (2023).

46. Y. Aoi, A. P. Shah, S. Ganesan, S. H. A. Soliman, B.-K. Cho, Y. A. Goo, N. L. Kelleher, A. Shilatifard, SPT6 functions in transcriptional pause/release via PAF1C recruitment. *Mol. Cell*. **82**, 3412–3423.e5 (2022).

47. N. Fong, R. M. Sheridan, S. Ramachandran, D. L. Bentley, The pausing zone and control of RNA polymerase II elongation by Spt5: Implications for the pause-release model. *Mol. Cell*. **82**, 3632–3645.e4 (2022).

48. W. Shao, J. Zeitlinger, Paused RNA polymerase II inhibits new transcriptional initiation.

Nat. Genet. **49**, 1045–1051 (2017).

49. C. Mylonas, C. Lee, A. L. Auld, I. I. Cisse, L. A. Boyer, A dual role for H2A.Z.1 in modulating the dynamics of RNA polymerase II initiation and elongation. *Nat. Struct. Mol. Biol.* **28**, 435–442 (2021).

50. S. A. Welsh, A. Gardini, Genomic regulation of transcription and RNA processing by the multitasking Integrator complex. *Nat. Rev. Mol. Cell Biol.* **24**, 204–220 (2023).

51. E. J. Wagner, L. Tong, K. Adelman, Integrator is a global promoter-proximal termination complex. *Mol. Cell*. **83**, 416–427 (2023).

52. H. Wang, Z. Fan, P. V. Shliaha, M. Miele, R. C. Hendrickson, X. Jiang, K. Helin, Publisher Correction: H3K4me3 regulates RNA polymerase II promoter-proximal pause-release. *Nature*. **616**, E7 (2023).

53. S. Hu, L. Peng, A. Song, Y.-X. Ji, J. Cheng, M. Wang, F. X. Chen, INTAC endonuclease and phosphatase modules differentially regulate transcription by RNA polymerase II. *Mol. Cell*. **83**, 1588–1604.e5 (2023).

54. I. Fianu, Y. Chen, C. Dienemann, O. Dybkov, A. Linden, H. Urlaub, P. Cramer, Structural basis of Integrator-mediated transcription regulation. *Science*. **374**, 883–887 (2021).

55. H. Zheng, Y. Qi, S. Hu, X. Cao, C. Xu, Z. Yin, X. Chen, Y. Li, W. Liu, J. Li, J. Wang, G. Wei, K. Liang, F. X. Chen, Y. Xu, Identification of Integrator-PP2A complex (INTAC), an RNA polymerase II phosphatase. *Science*. **370** (2020), doi:10.1126/science.abb5872.

56. K.-L. Huang, D. Jee, C. B. Stein, N. D. Elrod, T. Henriques, L. G. Mascibroda, D. Baillat, W. K. Russell, K. Adelman, E. J. Wagner, Integrator Recruits Protein Phosphatase 2A to Prevent Pause Release and Facilitate Transcription Termination. *Mol. Cell*. **80**, 345–358.e9 (2020).

57. S. Leidescher, J. Ribisel, S. Ullrich, Y. Feodorova, E. Hildebrand, A. Galitsyna, S. Bultmann, S. Link, K. Thanisch, C. Mulholland, J. Dekker, H. Leonhardt, L. Mirny, I. Solovei, Spatial organization of transcribed eukaryotic genes. *Nat. Cell Biol.* **24**, 327–339 (2022).

58. I. I. Cisse, I. Izeddin, S. Z. Causse, L. Boudarene, A. Senecal, L. Muresan, C. Dugast-Darzacq, B. Hajj, M. Dahan, X. Darzacq, Real-time dynamics of RNA polymerase II clustering in live human cells. *Science*. **341**, 664–667 (2013).

59. H. M. T. Choi, M. Schwarzkopf, M. E. Fornace, A. Acharya, G. Artavanis, J. Stegmaier, A. Cunha, N. A. Pierce, Third-generation in situ hybridization chain reaction: multiplexed, quantitative, sensitive, versatile, robust. *Development*. **145** (2018), doi:10.1242/dev.165753.

60. W. F. Marzluff, E. J. Wagner, R. J. Duronio, Metabolism and regulation of canonical histone mRNAs: life without a poly(A) tail. *Nat. Rev. Genet.* **9**, 843–854 (2008).

61. P. Quintero-Cadena, T. L. Lenstra, P. W. Sternberg, RNA Pol II Length and Disorder Enable Cooperative Scaling of Transcriptional Bursting. *Mol. Cell*. **79**, 207–220.e8 (2020).

62. F. Javier deHaro-Arbona, C. Roussos, S. Baloul, J. Townson, M. J. Gomez-Lamarca, S. Bray, Dynamic modes of Notch transcription hubs conferring memory and stochastic activation revealed by live imaging the co-activator Mastermind. *bioRxiv* (2023), p. 2023.08.10.552629.

63. A. Gardini, D. Baillat, M. Cesaroni, D. Hu, J. M. Marinis, E. J. Wagner, M. A. Lazar, A. Shilatifard, R. Shiekhattar, Integrator regulates transcriptional initiation and pause release following activation. *Mol. Cell*. **56**, 128–139 (2014).

64. B. Stadelmayer, G. Micas, A. Gamot, P. Martin, N. Malirat, S. Koval, R. Raffel, B. Sobhian, D. Severac, S. Rialle, H. Parrinello, O. Cuvier, M. Benkirane, Integrator complex regulates NELF-mediated RNA polymerase II pause/release and processivity at coding genes. *Nat. Commun.* **5**, 5531 (2014).

65. F. Beckedorff, E. Blumenthal, L. F. daSilva, Y. Aoi, P. R. Cingaram, J. Yue, A. Zhang, S. Dokaneheifard, M. G. Valencia, G. Gaidosh, A. Shilatifard, R. Shiekhattar, The Human Integrator Complex Facilitates Transcriptional Elongation by Endonucleolytic Cleavage of Nascent Transcripts. *Cell Rep.* **32**, 107917 (2020).

66. N. D. Elrod, T. Henriques, K.-L. Huang, D. C. Tatomer, J. E. Wilusz, E. J. Wagner, K. Adelman, The Integrator Complex Attenuates Promoter-Proximal Transcription at Protein-Coding Genes. *Mol. Cell*. **76**, 738–752.e7 (2019).

67. D. C. Tatomer, N. D. Elrod, D. Liang, M.-S. Xiao, J. Z. Jiang, M. Jonathan, K.-L. Huang, E. J. Wagner, S. Cherry, J. E. Wilusz, The Integrator complex cleaves nascent mRNAs to attenuate transcription. *Genes Dev.* **33**, 1525–1538 (2019).

68. C. B. Stein, A. R. Field, C. A. Mimoso, C. Zhao, K.-L. Huang, E. J. Wagner, K. Adelman, Integrator endonuclease drives promoter-proximal termination at all RNA polymerase II-transcribed loci. *Mol. Cell*. **82**, 4232–4245.e11 (2022).

69. G. W. Muse, D. A. Gilchrist, S. Nechaev, R. Shah, J. S. Parker, S. F. Grissom, J. Zeitlinger, K. Adelman, RNA polymerase is poised for activation across the genome. *Nat. Genet.* **39**, 1507–1511 (2007).

70. M. Levine, Paused RNA polymerase II as a developmental checkpoint. *Cell*. **145**, 502–511 (2011).

71. K. Adelman, J. T. Lis, Promoter-proximal pausing of RNA polymerase II: emerging roles in metazoans. *Nat. Rev. Genet.* **13**, 720–731 (2012).

72. B. Gaertner, J. Zeitlinger, RNA polymerase II pausing during development. *Development*. **141**, 1179–1183 (2014).

73. R. Dollinger, D. S. Gilmour, Regulation of Promoter Proximal Pausing of RNA Polymerase

II in Metazoans. *J. Mol. Biol.* **433**, 166897 (2021).

74. M. Noe Gonzalez, D. Blears, J. Q. Svejstrup, Causes and consequences of RNA polymerase II stalling during transcript elongation. *Nat. Rev. Mol. Cell Biol.* **22**, 3–21 (2021).

75. A. Abuhashem, V. Garg, A.-K. Hadjantonakis, RNA polymerase II pausing in development: orchestrating transcription. *Open Biol.* **12**, 210220 (2022).

76. J. B. Grimm, B. P. English, J. Chen, J. P. Slaughter, Z. Zhang, A. Revyakin, R. Patel, J. J. Macklin, D. Normanno, R. H. Singer, T. Lionnet, L. D. Lavis, *Nat. Methods*, in press, doi:10.1038/nmeth.3256.

77. Y. Chen, N. Kotian, J. A. McDonald, Quantitative Image Analysis of Dynamic Cell Behaviors During Border Cell Migration. *Methods Mol. Biol.* **2626**, 193–217 (2023).

78. T. U. Banisch, I. Maimon, T. Dadosh, L. Gilboa, Escort cells generate a dynamic compartment for germline stem cell differentiation via combined Stat and Erk signalling. *Development*. **144**, 1937–1947 (2017).

79. Y. Qiu, D. S. Gilmour, Identification of Regions in the Spt5 Subunit of DRB Sensitivity-inducing Factor (DSIF) That Are Involved in Promoter-proximal Pausing. *J. Biol. Chem.* **292**, 5555–5570 (2017).

80. E. D. Andrulis, E. Guzmán, P. Döring, J. Werner, J. T. Lis, High-resolution localization of Drosophila Spt5 and Spt6 at heat shock genes in vivo: roles in promoter proximal pausing and transcription elongation. *Genes Dev.* **14**, 2635–2649 (2000).

81. K. Hanyu-Nakamura, H. Sonobe-Nojima, A. Tanigawa, P. Lasko, A. Nakamura, Drosophila Pgc protein inhibits P-TEFb recruitment to chromatin in primordial germ cells. *Nature*. **451**, 730–733 (2008).

82. R. Fujiwara, S.-N. Zhai, D. Liang, M. Tracey, X.-K. Ma, A. P. Shah, C. J. Fields, M. S. Mendoza-Figueroa, M. C. Meline, D. C. Tatomer, L. Yang, J. E. Wilusz, IntS6 and the Integrator phosphatase module tune the efficiency of select premature transcription termination events. *bioRxiv* (2023), p. 2023.03.05.531184.

83. X. Long, J. Colonell, A. M. Wong, R. H. Singer, T. Lionnet, Quantitative mRNA imaging throughout the entire Drosophila brain. *Nat. Methods*. **14**, 703–706 (2017).

84. J. Schindelin, I. Arganda-Carreras, E. Frise, V. Kaynig, M. Longair, T. Pietzsch, S. Preibisch, C. Rueden, S. Saalfeld, B. Schmid, J.-Y. Tinevez, D. J. White, V. Hartenstein, K. Eliceiri, P. Tomancak, A. Cardona, Fiji: an open-source platform for biological-image analysis. *Nat. Methods*. **9**, 676–682 (2012).

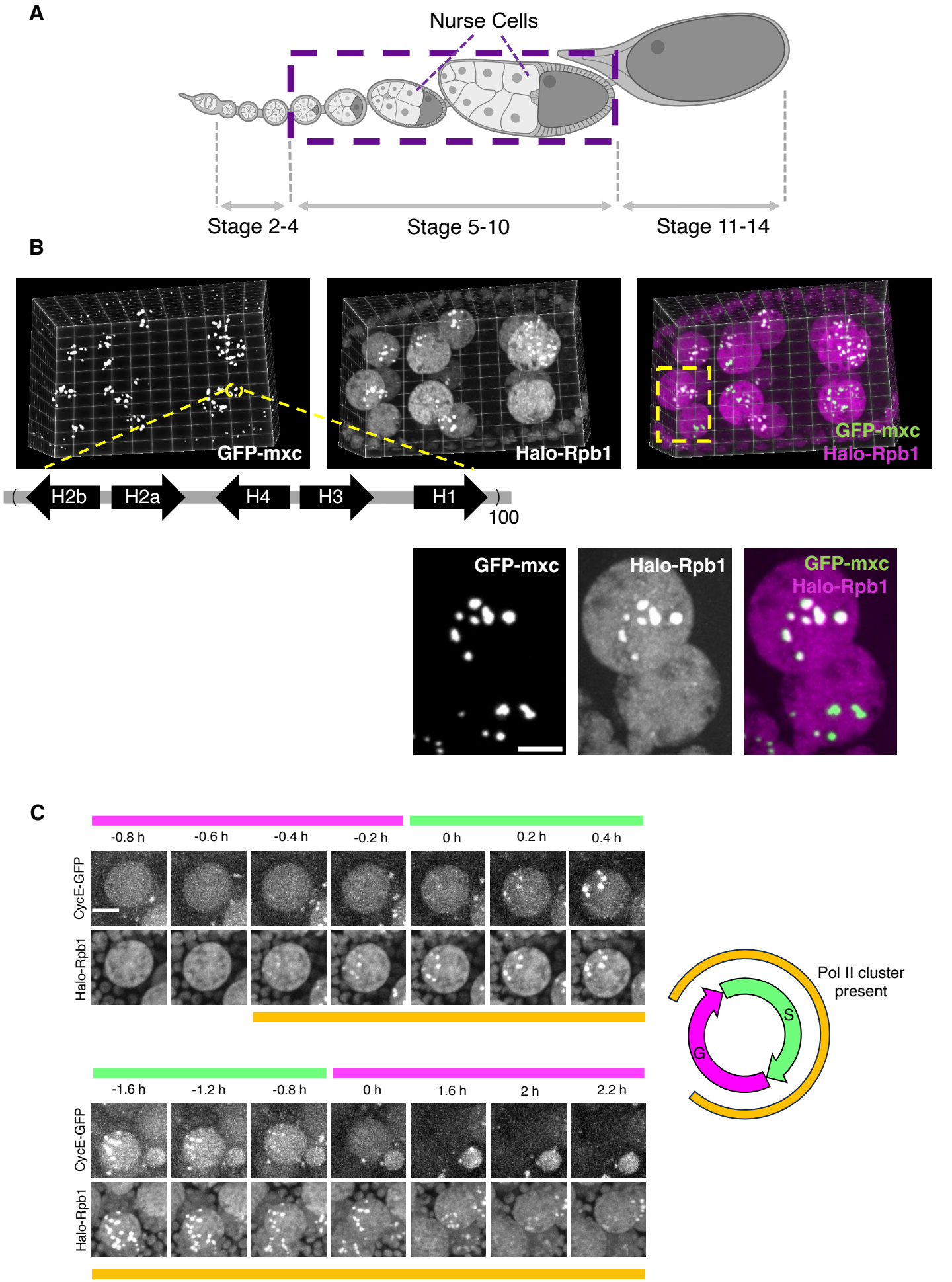
A
Nurse Cells
Stage 2-4
Stage 5-10
Stage 11-14
B
GFP-mxc
Halo-Rpb1
GFP-mxc
Halo-Rpb1
H2b
H2a
H4
H3
H1
100
GFP-mxc
Halo-Rpb1
GFP-mxc
Halo-Rpb1
C
-0.8 h
-0.6 h
-0.4 h
-0.2 h
0 h
0.2 h
0.4 h
CycE-GFP
Halo-Rpb1
-1.6 h
-1.2 h
-0.8 h
0 h
1.6 h
2 h
2.2 h
CycE-GFP
Halo-Rpb1
Pol II cluster present
S
G

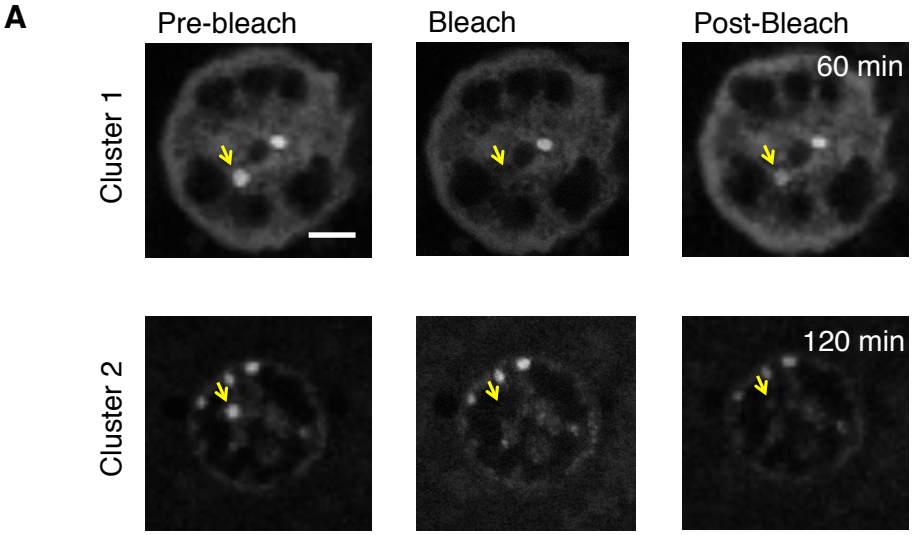
A
Pre-bleach
Bleach
Post-Bleach
60 min
Cluster 1
Cluster 2
120 min

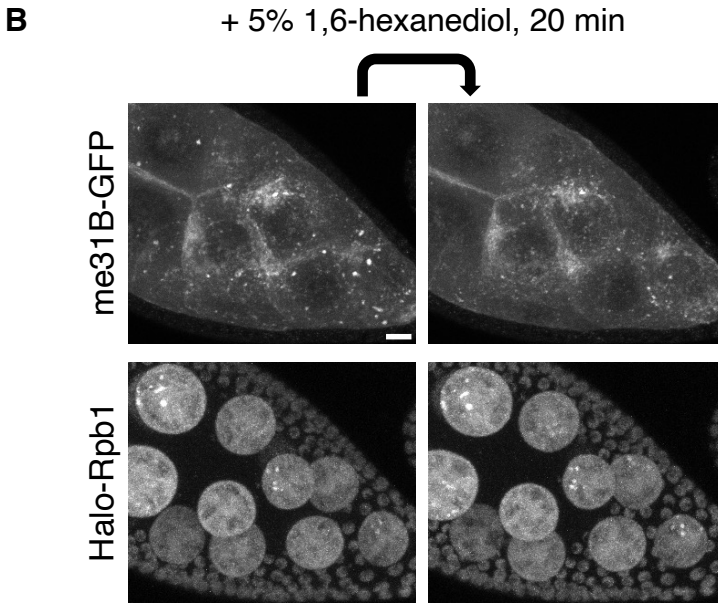
B
+ 5% 1,6-hexanediol, 20 min
me31B-GFP
Halo-Rpb1

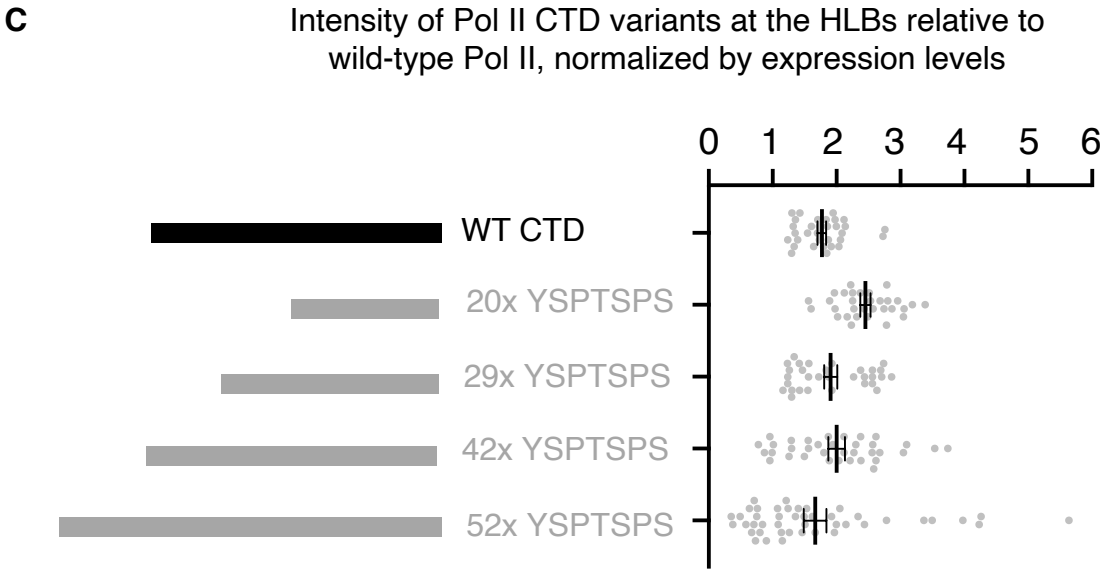
C
Intensity of Pol II CTD variants at the HLBs relative to wild-type Pol II, normalized by expression levels
0
1
2
3
4
5
6
WT CTD
20x YSPTSPS
29x YSPTSPS
42x YSPTSPS
52x YSPTSPS

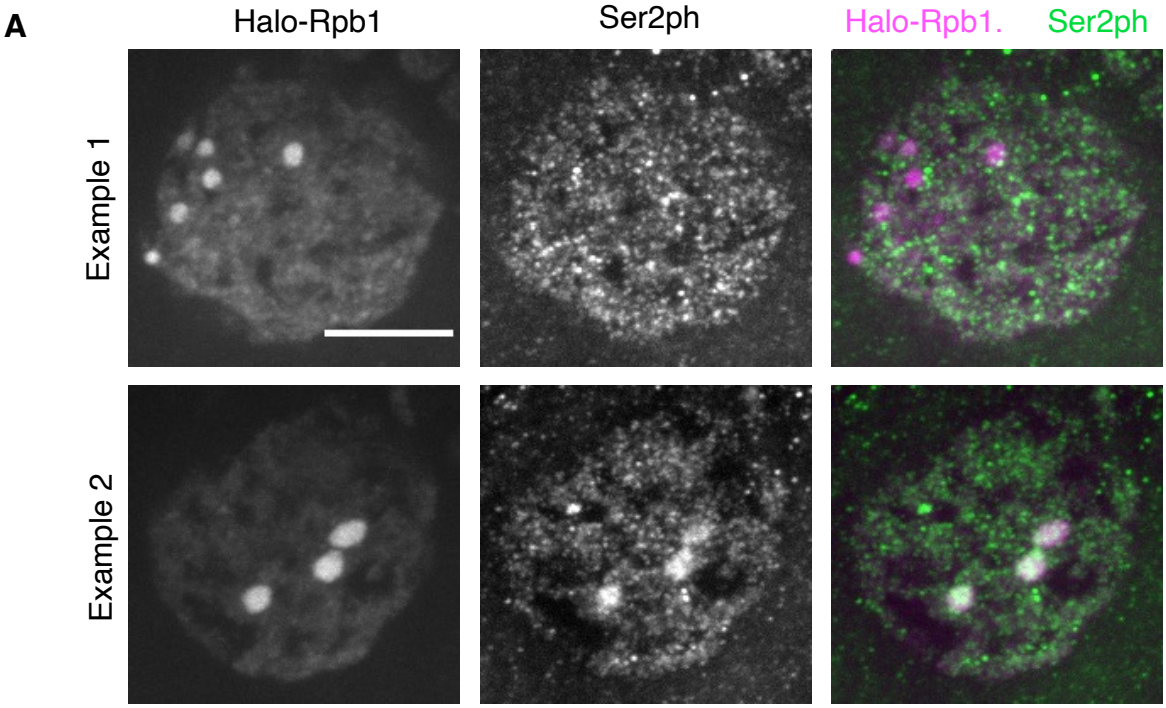
A
Halo-Rpb1
Ser2ph
Halo-Rpb1.
Ser2ph
Example 1
Example 2

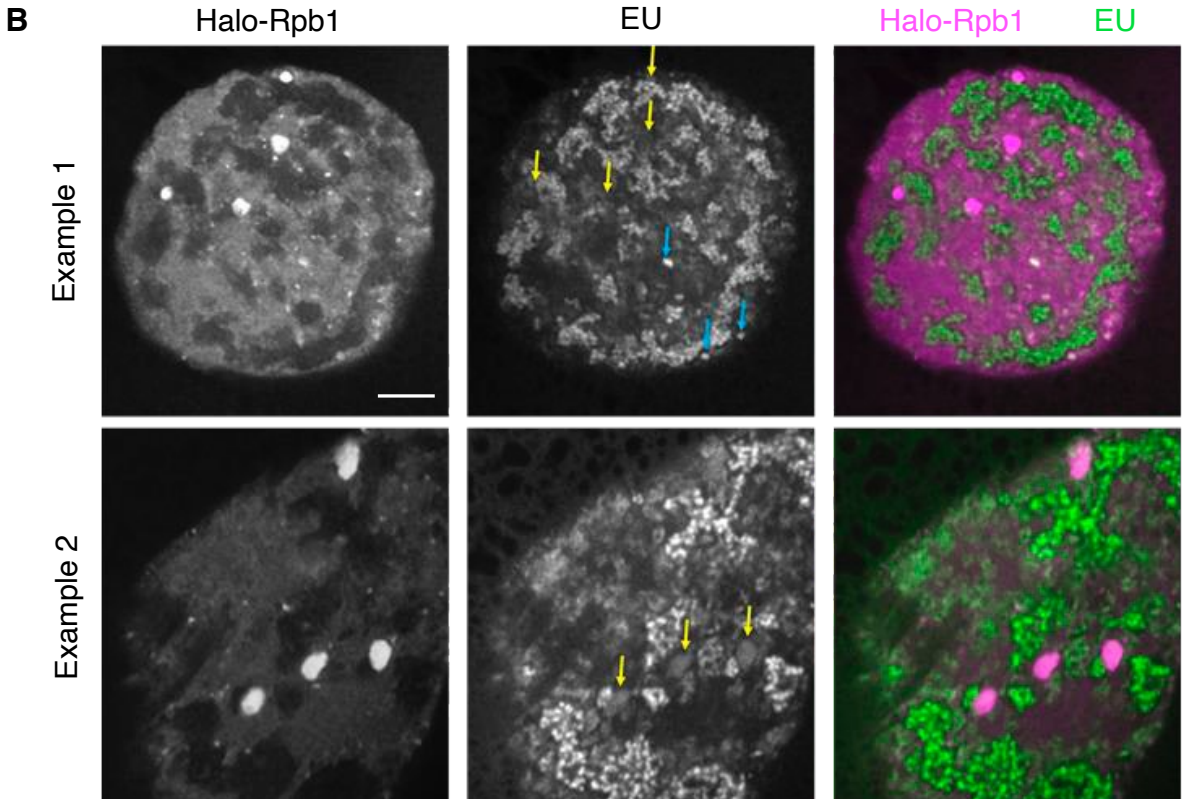
B
Halo-Rpb1
EU
Halo-Rpb1
EU
Example 1
Example 2

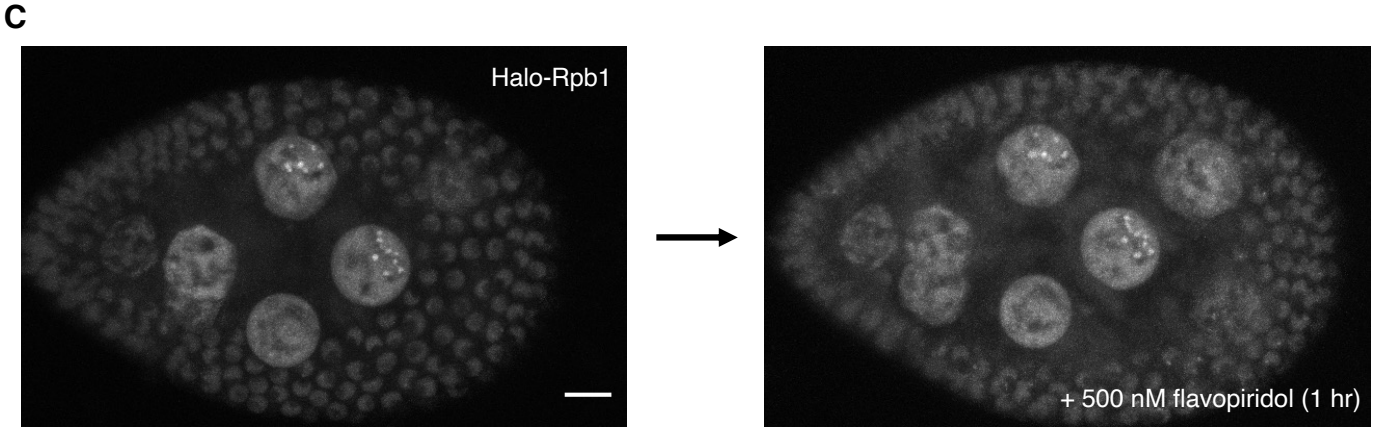
C
Halo-Rpb1
+ 500 nM flavopiridol (1 hr)

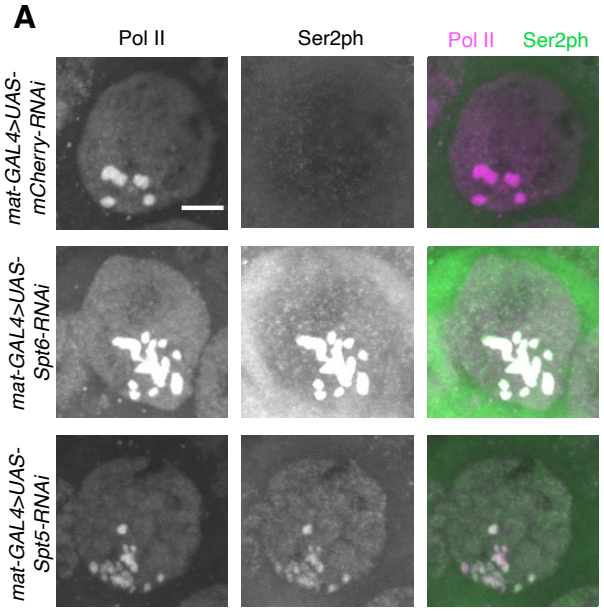
A
Pol II
Ser2ph
Pol II
Ser2ph
mat-GAL4>UAS-mCherry-RNAi
mat-GAL4>UAS-Spt6-RNAi
mat-GAL4>UAS-Spt5-RNAi

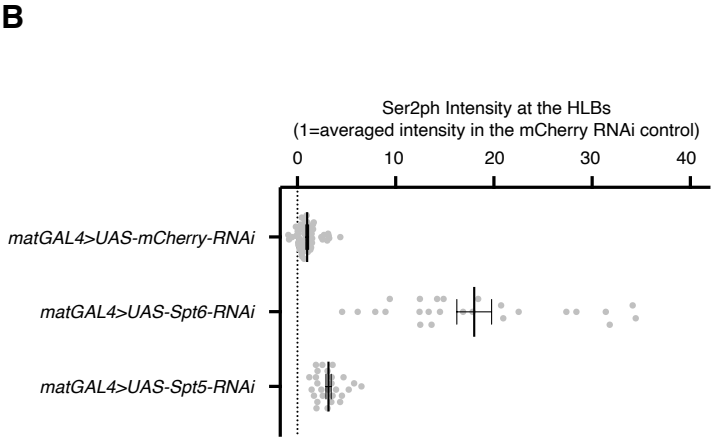
B
Ser2ph Intensity at the HLBs
(1=averaged intensity in the mCherry RNAi control)
0
10
20
30
40
matGAL4>UAS-mCherry-RNAi
matGAL4>UAS-Spt6-RNAi
matGAL4>UAS-Spt5-RNAi

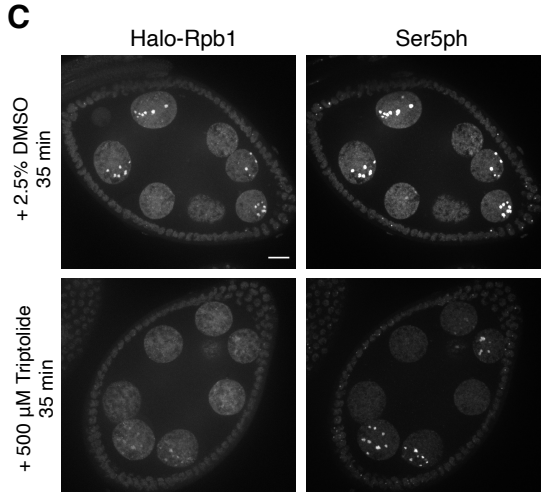
C
Halo-Rpb1
Ser5ph
+ 2.5% DMSO
35 min
+ 500 µM Triptolide
35 min

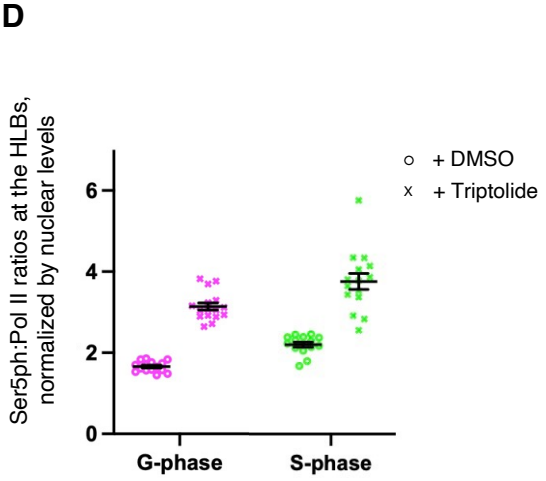
D
Ser5ph:Pol II ratios at the HLBs,
normalized by nuclear levels
0
2
4
6
+ DMSO
+ Triptolide
G-phase
S-phase

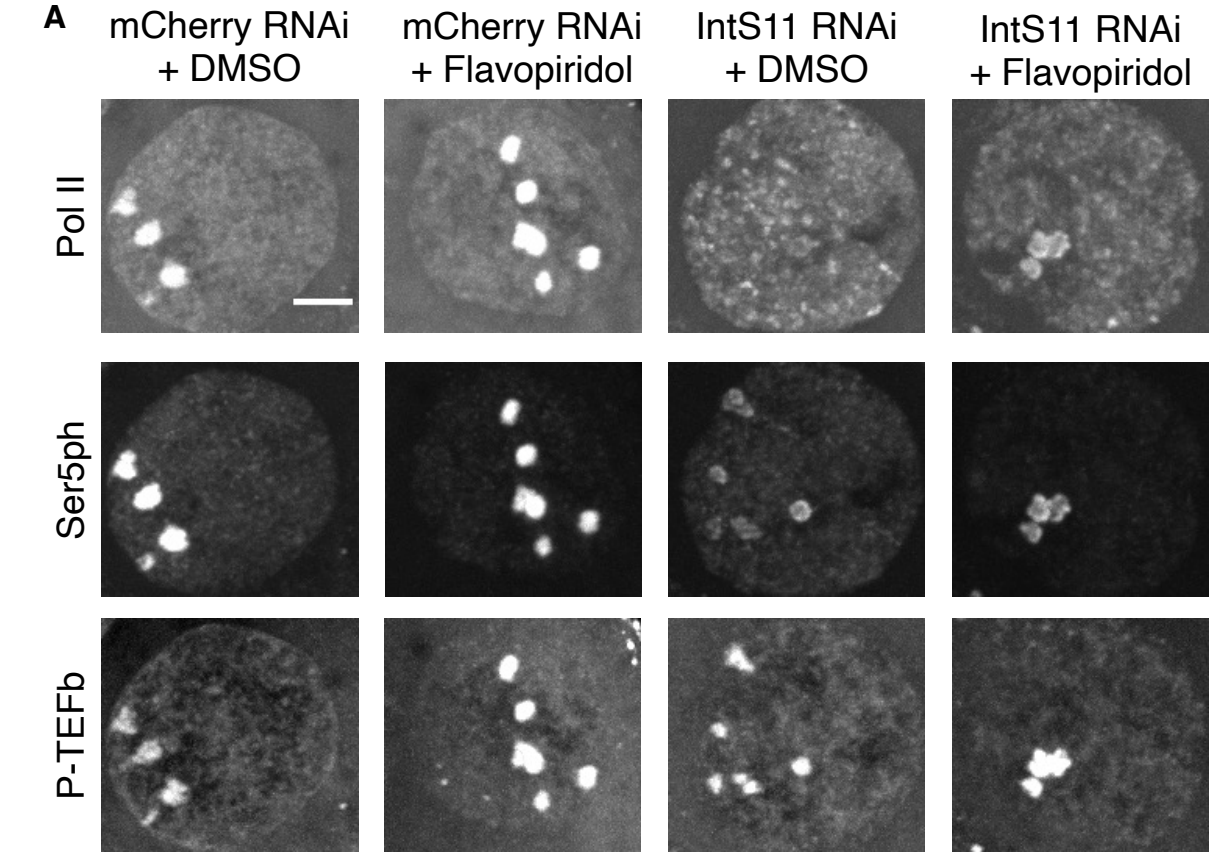
A
mCherry RNAi + DMSO
mCherry RNAi + Flavopiridol
IntS11 RNAi + DMSO
IntS11 RNAi + Flavopiridol
Pol II
Ser5ph
P-TEFb

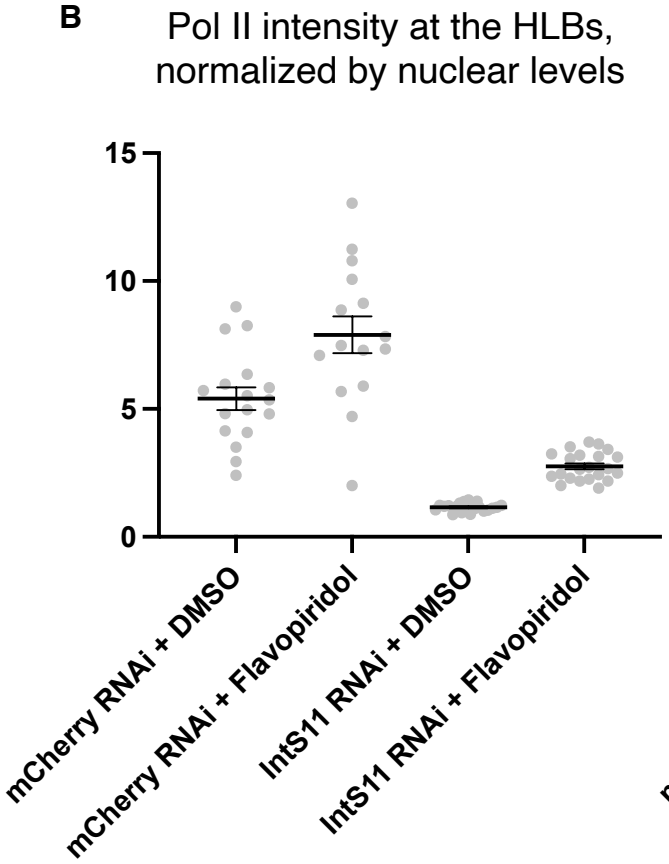
B
Pol II intensity at the HLBs, normalized by nuclear levels
15
10
5
0
mCherry RNAi + DMSO
mCherry RNAi + Flavopiridol
IntS11 RNAi + DMSO
IntS11 RNAi + Flavopiridol

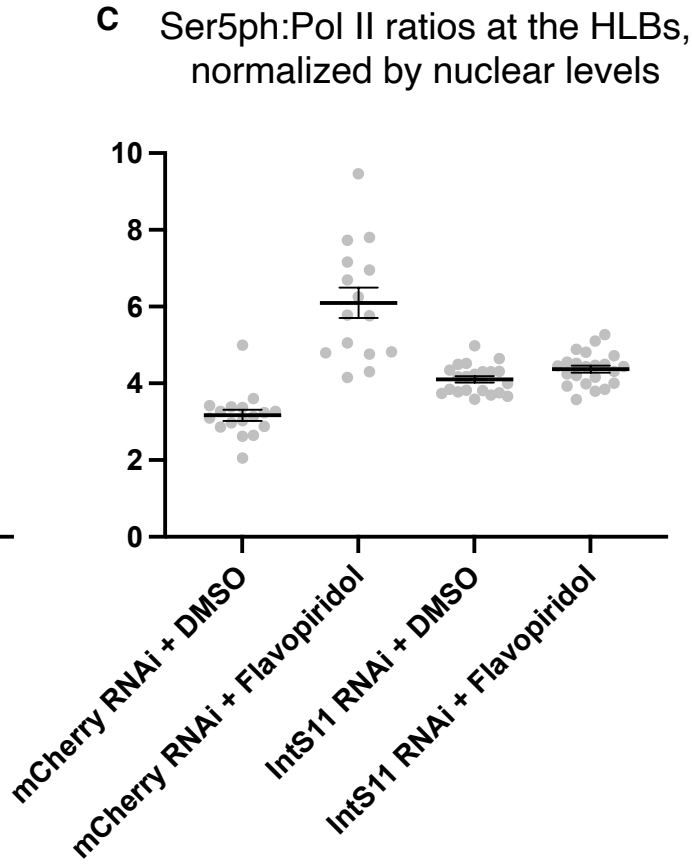
C
Ser5ph:Pol II ratios at the HLBs, normalized by nuclear levels
10
8
6
4
2
0
mCherry RNAi + DMSO
mCherry RNAi + Flavopiridol
IntS11 RNAi + DMSO
IntS11 RNAi + Flavopiridol

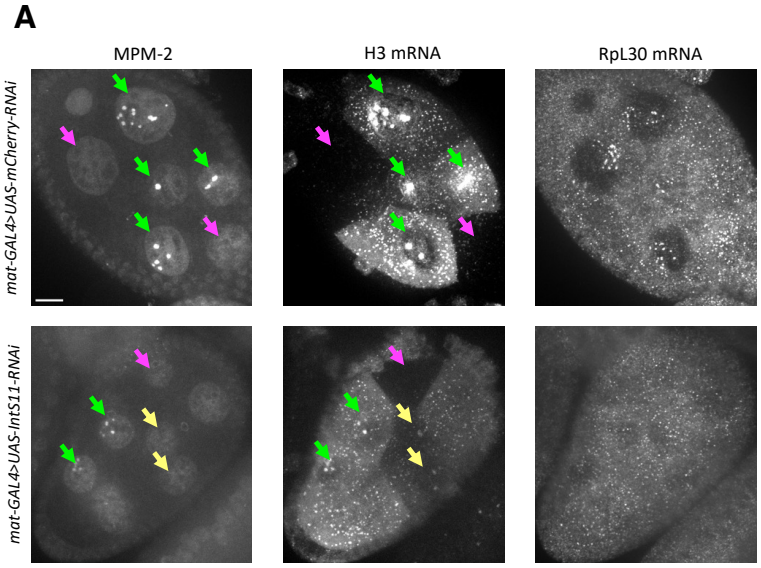
A
MPM-2
H3 mRNA
RpL30 mRNA
mat-GAL4>UAS-mCherry-RNAi
mat-GAL4>UAS-IntS11-RNAi

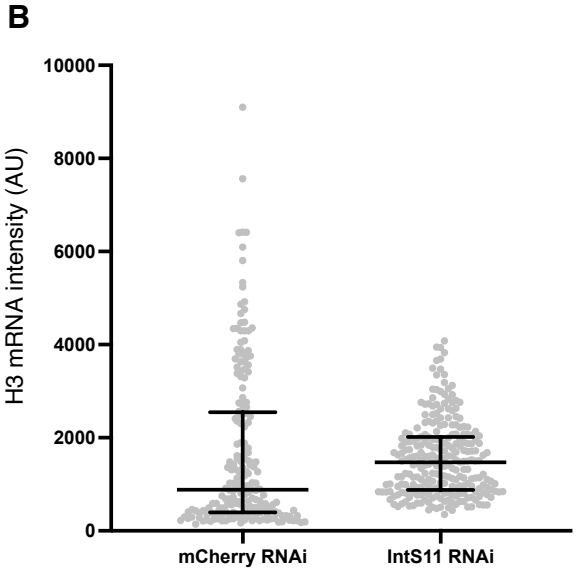
B
H3 mRNA intensity (AU)
10000
8000
6000
4000
2000
0
mCherry RNAi
IntS11 RNAi

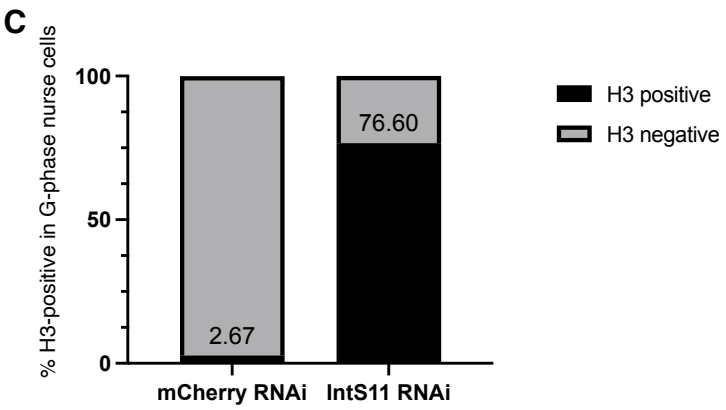
C
% H3-positive in G-phase nurse cells
100
50
0
2.67
76.60
mCherry RNAi
IntS11 RNAi
H3 positive
H3 negative

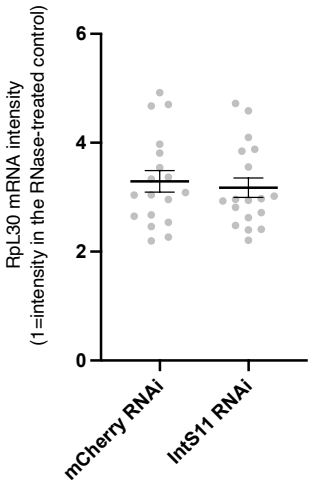
D
RpL30 mRNA intensity
(1=intensity in the RNase-treated control)
6
4
2
0
mCherry RNAi
IntS11 RNAi

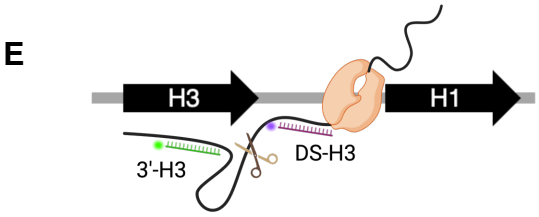
E
H3
H1
3'-H3
DS-H3

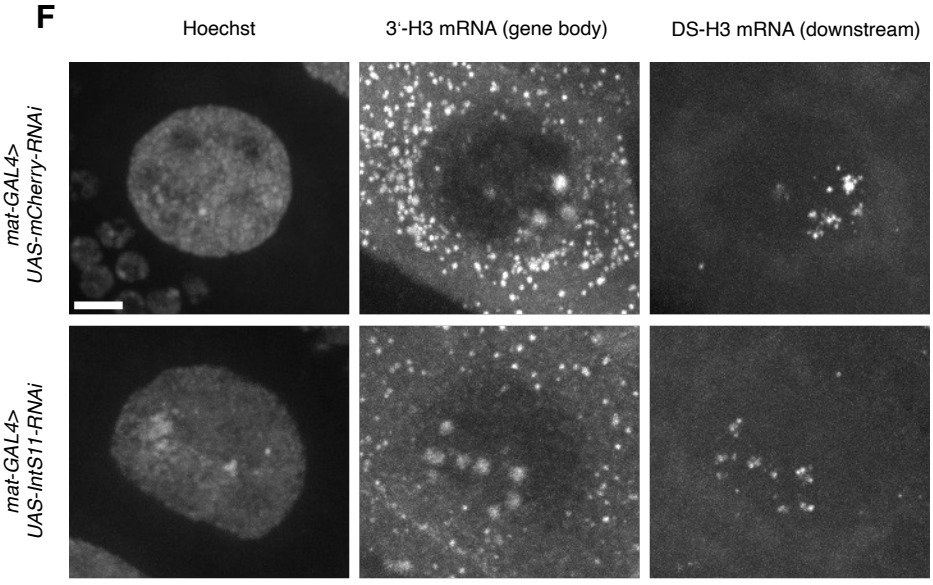
F
Hoechst
3'-H3 mRNA (gene body)
DS-H3 mRNA (downstream)
mat-GAL4>
UAS-mCherry-RNAi
mat-GAL4>
UAS-IntS11-RNAi

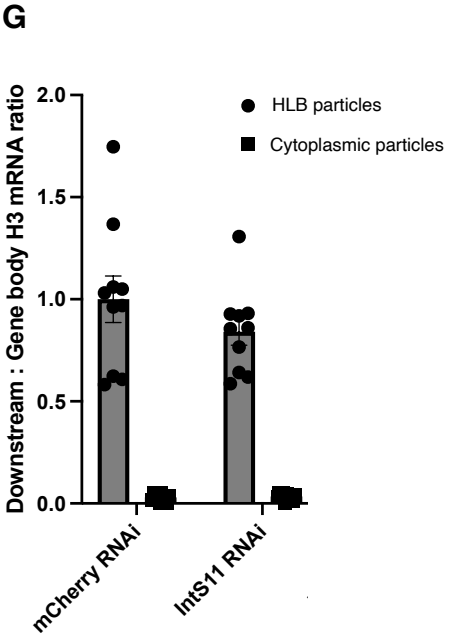
G
Downstream : Gene body H3 mRNA ratio
2.0
1.5
1.0
0.5
0.0
HLB particles
Cytoplasmic particles
mCherry RNAi
IntS11 RNAi

With IntS11/IntS9

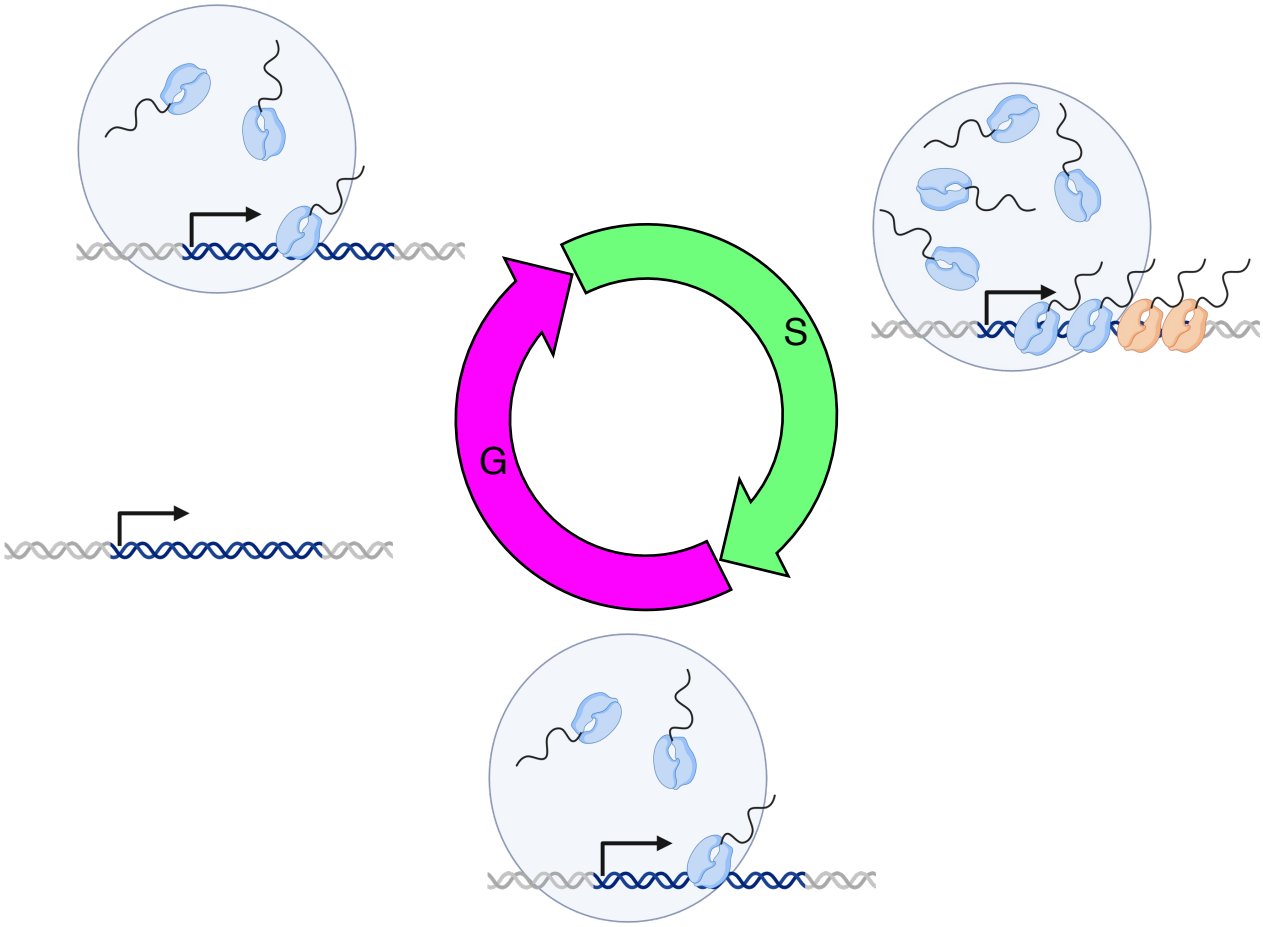
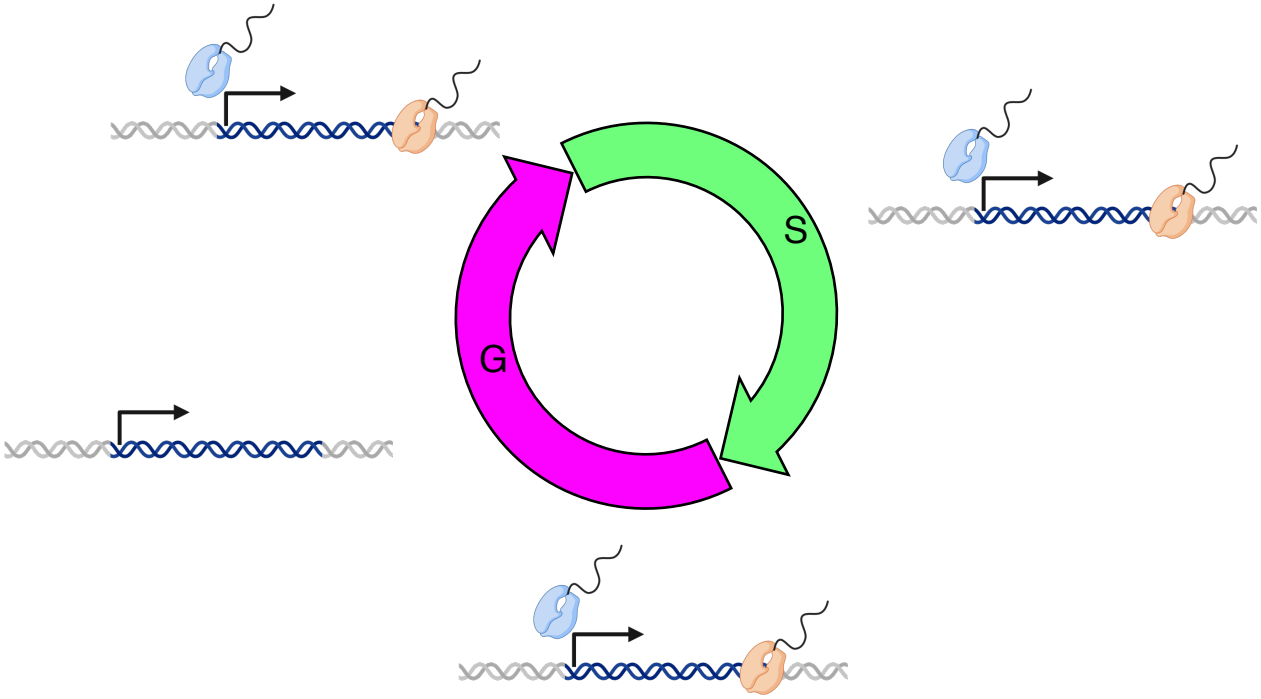
Without IntS11/IntS9